Mechanics of Advanced Materials and Structures (2015) **22**, 717–721

ISSN: 1537-6494 print / 1537-6532 online
DOI: 10.1080/15376494.2013.839067

Taylor & Francis
Taylor & Francis Group

A Density Functional Theory Study of the Mechanical Properties of Graphane With van der Waals Corrections

QING PENG[1], ZHONGFANG CHEN[2], and SUVRANU DE[1]

[1]*Department of Mechanical, Aerospace and Nuclear Engineering, Rensselaer Polytechnic Institute, Troy, New York, USA*
[2]*Department of Chemistry, Institute for Functional Nanomaterials, University of Puerto Rico, San Juan, Puerto Rico*

Received 14 May 2013; accepted 6 August 2013.

We investigate the mechanical properties of graphane using first-principles calculations based on density functional theory (DFT) with van der Waals (vdW) interactions in DFT-D2 approach. The mechanical stability of graphane was tested with three deformation modes — armchair, zigzag, and biaxial. We find that it is safe to neglect vdW because it has little effect on the geometry ($<0.4\%$) and the mechanical properties, including ultimate stresses (2%), ultimate strains (8.7%), in-plane stiffness (1%), and Poisson ratio (3%). Our result is helpful to estimate the effect of vdW on the mechanical properties of chemically functionalized graphane systems.

Keywords: carbon materials, elastic properties, deformation and fracture, density functional theory, high-order elastic constants, van der Waals interactions

1. Introduction

The van der Waals (vdW) interactions [1, 2] play a critical role in predicting the properties of graphene based systems using first-principles studies, including graphene on metals [3], molecules [4], bilayers [5], hydrogen adsorption [6], and functionalization [7]. Since van der Waals forces are relatively weak compared to covalent bonds, in general their contribution to the elastic constants of bulk crystalline is negligible. In hydrogen functionalized graphene, the unbonded hydrogen atoms are very close, 2.54 Å in graphane for example [8–10]. Because the van der Waals forces increase rapidly (in a form of R^{-6}) with the decreasing of the separation of atoms R, the vdW interactions between hydrogen atoms in graphane might contribute to the mechanical properties to some extent, which is thought to be small, but the accurate knowledge is still unknown.

Mechanical properties are critical in engineering design regarding the practical applications. For example, strain engineering is a common, important, and effective approach to tailor the functional and structural properties of the nanomaterials [11], including strain-based electronics [12] due to its relative simplicity in controlling and "clean" without changing the chemistry. Therefore, accurate knowledge of mechanical properties of graphane is highly desired.

The goal of this article is to quantify the effect of the van der Waals interactions on the mechanical properties of graphane, the full hydrogen functionalized graphene, through a comparative study using first-principles simulations based on the density functional theory (DFT) with and without van der Waals interactions in DFT-D2 approach [2]. This study is very useful to estimate the effect of van der Waals interactions on the mechanical properties of a large class of chemically functionalized graphene systems, including those with *s*-type, *p*-type, and *d*-type functionalization chemicals [13–16], predicted from van der Waals density functional calculations.

Hydrogenation is a chemical modification towards opening the bandgap of graphene [8]. As a derivative of graphene, graphane [17–19] is a theoretical nonmagnetic semiconductor with an energy gap formed by 100% hydrogenation of graphene, which can be reversed and the original properties restored by annealing graphane at high temperatures [20], making graphane a viable option for hydrogen storage materials [21]. Precise knowledge of the mechanical properties of graphane is indispensable in consideration of its applications. It turns out that such hydrogenation greatly reduces the stiffness by about 30% [22] compared to graphene, one of the strongest materials ever tested with a tensile modulus of 1 TPa [23]. The second order elastic constants (in-plane Young's modulus, and Poisson's ratio) have been reported [22, 24–26], as well as the higher order elastic constants [27], which are needed when the atomic displacement is no longer small with respect to the interatomic spacing [28].

Address correspondence to Qing Peng, Department of Mechanical, Aerospace and Nuclear Engineering, Rensselaer Polytechnic Institute, 110 8th Street, JEC 2303, Troy, NY 12180, USA. E-mail: qpeng.org@gmail.com
Color versions of one or more of the figures in the article can be found online at www.tandfonline.com/umcm.

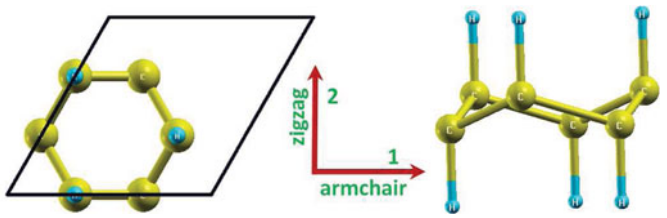

Fig. 1. Top view (left) and side view (right) of the simulation box of graphane (12 atoms) in the undeformed reference configuration.

2. Computational Method

We consider a conventional unit cell, which contains 6 carbon atoms for graphene and 12 atoms (6 carbon atoms and 6 hydrogen atoms) for graphane (Figure 1), with periodic boundary conditions. DFT calculations were carried out with the Vienna Ab-initio Simulation Package (VASP)[29] which is based on the Kohn-Sham Density Functional Theory (KS-DFT)[30] with the generalized gradient approximations as parameterized by Perdew, Burke, and Ernzerhof (PBE) for exchange-correlation functions [31]. The electrons explicitly included in the calculations are the ($2s^2 2p^2$) electrons for carbon atoms and 1s for hydrogen atoms. The core electrons ($1s^2$) of carbon atoms are replaced by the projector augmented wave (PAW) and pseudo-potential approach [32] A plane-wave cutoff of 600 eV and a Gamma-centered $25 \times 25 \times 1$ k-mesh are used in all the calculations. There was a 15-Å-thick vacuum region to reduce the inter-layer interaction to model the single layer system. The total energies and forces are converged to 0.000001 eV and 0.001 eV/Å, respectively. The calculations are performed at zero temperature. The van der Waals interactions are described via a simple pair-wise force field in the DFT-D2 method of Grimme [2]. The parameters are $C_6 = 1.75$ Jnm^6/mol and $R_0 = 1.452$ Å for carbon, and $C_6 = 0.14$ Jnm^6/mol and $R_0 = 1.001$ Å for hydrogen. The cutoff radius for pair interactions is 30.00 Å . The global scaling factor of 0.75 and damping parameter of 20.0 are implemented. The atomic structures of all the deformed and undeformed configurations were obtained by fully relaxing all atoms in the unit cells. To eliminate the artificial effect of the out-of-plane thickness of the simulation box on the stress, we used the second Piola–Kirchhoff stress [33] to express the 2D forces per unit length with units of N/m.

By a two-step least-squares fit, the 14 independent elastic constants are obtained from stress-strain relationships, which are calculated by DFT-based first-principles studies [34–44]. In the first step, we use a least-squares fit of stress-strain formula from elastic theory [33] into five stress-strain responses of the graphane from DFT calculations. Five relationships between stress and strain are necessary because there are five independent components in fifth-order elastic constants. We obtain the stress-strain relationships by simulating the following deformation states: uni-axial strain in the zigzag direction (zigzag); uni-axial strain in the armchair direction (armchair); and equibiaxial strain (biaxial). From the first step, the components of the second-order elastic constants (SOEC), the third-order elastic constants (TOEC), and the fourth-order elastic constants (FOEC) are *over*-determined (i.e., the number of linearly independent variables is *greater* than the number of constraints), and the fifth-order elastic constants (FFOEC) are *well*-determined (the number of linearly independent variables is *equal* to the number of constraints). Under such circumstances, a second step is needed: a least-square solution to these over- and well-determined linear equations.

3. Results and Analysis

The most energetically favorable structure is set as the strain-free structure. The six carbon atoms in the unitcell of graphane are in double planes (Figure 1, right), opposite to co-plane configuration in graphene, due to different bonding types of carbon atoms: sp^3 in graphane but sp^2 in graphene [48]. Without considering the van der Waals interactions (i.e., *DFT*), the bond length of the C–C bond in graphane is 1.537 Å, which is only 0.004 Å (or 0.3%) longer than that predicted by *DFT-D2*. The C–H bond length, the distance between the two carbon planes δ_{CC}, the C–C–C angle γ_{C-C-C}, and the C–C–H angle γ_{C-C-H} are listed in Table 1. As a calibration, our *DFT* results are in good agreement with previous DFT calculations [24, 26, 49]. It is not surprising that the graphane structure is similar to a diamond structure (C–C bond length 1.54 Å, bond angle 120°and 109.5°), since the carbons have the same type of (sp^3) bonds. Our results of the *DFT-D2* calculations indicates that the van der Waals interactions have little effect on the geometry of graphane, less than 0.4%.

The second P-K stress versus Lagrangian strain relationship for uniaxial strains along the armchair and zigzag directions and biaxial strains, predicted from both *DFT-D2* and *DFT*, are shown in Figure 2. It is clear that the van der Waals interactions have little effect on the stress-strain responses of graphane, as the two curves are nearly identical.

It is worthy to note that the systems of perfect graphane under strains beyond the ultimate strains (corresponding strain

Table 1. Geometry parameters of graphane in the strain-free state, ultimate strengths (Σ_m^a,Σ_m^z,Σ_m^b), and ultimate strains (η_m^a, η_m^z, η_m^b) predicted by *DFT-D2* compared with *DFT* calculations of graphane and graphene [27].

	DFT-D2	*DFT*	Graphene [27]
a (Å)	2.532	2.541	2.468
d_{C-C} (Å)	1.533	1.537	1.425
d_{C-H} (Å)	1.111	1.111	—
δ_{CC} (Å)	0.460	0.459	0
γ_{C-C-H} (°)	107.45	107.37	—
γ_{C-C-C} (°)	111.39	111.49	120
Σ_m^a (N/m)	19.1	18.9	28.6
η_m^a	0.17	0.17	0.19
Σ_m^z (N/m)	21.8	21.4	30.4
η_m^z	0.25	0.25	0.23
Σ_m^b (N/m)	21.2	20.8	32.1
η_m^b	0.25	0.23	0.23

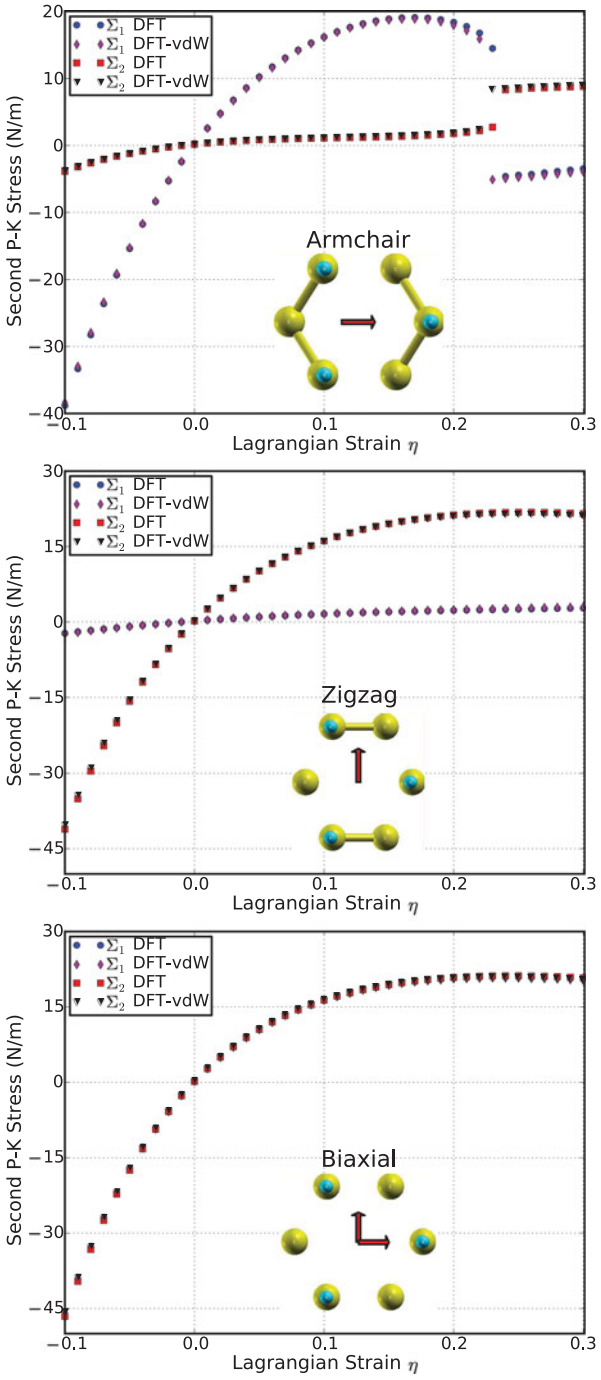

Fig. 2. Stress-strain responses of graphane predicted from *DFT-D2* and *DFT* under the armchair, zigzag, and biaxial strain. Σ_1 (Σ_2) denotes the x (y) component of stress.

at maximum stress) are in a metastable state, which can be easily destroyed by long wavelength perturbations and vacancy defects, as well as high temperature effects [22]. The ultimate strain is determined by the intrinsic bonding strengths and acts as a lower limit of the critical strain. Thus, it has practical meaning in consideration for its applications. As a result, only the data within the ultimate strain was used to determine the high order elastic constants.

The ultimate strengths and strains corresponding to the various strain conditions are summarized in Table 1. The ultimate stresses from *DFT-D2* calculations are 1.06, 1.87, and 1.92% larger than those from *DFT* calculations in armchair, zigzag, and biaxial deformations respectively. The ultimate strain in biaxial deformations from *DFT-D2* calculations is 8.7% larger than that from *DFT* calculations. However, those in armchair and zigzag deformations have no difference with van der Waals interactions. These results illustrate that the van der Waals interactions have little effect on the ultimate strengths and strains of graphane.

The material behaves in an asymmetric manner with respect to compressive and tensile strains. With increasing strains, the C–C bonds are stretched and eventually rupture. The insets in Figure 2 shows the atomic structure of graphane at ultimate strain. When the strain is applied in the armchair direction, the bonds of those parallel in this direction are more severely stretched than those in other directions. The C–H bonds are not affected since they are perpendicular to the strains. Under the deformation mode z, in which the strain is applied perpendicular to the armchair, there is no bond parallel to this direction. The bonds inclined to the zigzag direction with an angle of 30° are more severely stretched than those in the armchair direction. Under the ultimate strain in mode z, which is 0.25, the bonds inclined to the armchair direction are observed to be ruptured (Figure 2b). Under the ultimate strain in mode b ($\eta_m^b = 0.25$), all the C–C bonds are observed to be ruptured (Figure 2c)

The elastic constants (Table 2) are critical parameters for mechanical properties of materials. Our results for these elastic constants provide an accurate continuum description of the elastic properties of graphane from ab initio density

Table 2. Nonzero independent components for the SOEC, TOEC, FOEC, and FFOEC tensor components, in-plane stiffness Y_s (in units of N/m), and Poisson's ration ν of graphane from *DFT-D2* calculations, compared to the *DFT* calculations of graphane and graphene [27].

	DFT-D2	*DFT*	Graphane [24][a]	Graphene [27]
Y_s	249.3	246.7	246.4	340.8
ν	0.076	0.078	0.081	0.178
C_{11}	250.8	248.2	248	352.0
C_{12}	19.1	19.4	20	62.6
C_{111}	−2433.0	−2374.1	−1385	−3089.7
C_{112}	−94.7	−95.4	−195	−453.8
C_{222}	−2211.1	−2162.8		−2928.1
C_{1111}	20,492	19,492		21,927
C_{1112}	513	819		2731
C_{1122}	271	68		3888
C_{2222}	14,815	14,823		18,779
C_{11111}	−11,0821	−10,3183		−11,8791
C_{11112}	2215	816		−19,173
C_{11122}	−13,239	−16,099		−15,863
C_{12222}	−12,955	−10,151		−27,463
C_{22222}	−118,064	−134,277		−134,752

[a] 4-atom unitcell (two C and two H atoms).

functional theory calculations. They are suitable for incorporation into numerical methods, such as the finite element technique.

The in-plane Young's modulus Y_s and Poisson's ratio ν are obtained from the following relationships: $Y_s = (C_{11}^2 - C_{12}^2)/C_{11}$ and $\nu = C_{12}/C_{11}$. Without vdW, our results for graphane are $Y_s = 246.7$ (N/m) and $\nu = 0.078$ which are in good agreement with a previous *ab initio* study ($Y_s = 243$ (N/m) and $\nu = 0.07$) [22, 24]. The introduction of the van der Waals interactions does not change the results much.

Table 2 summarized our results and compared to graphene and other *DFT* calculations, which indicates that the van der Waals interactions have little effect on the other elastic constants too. Particularly, with vdW, the in-plane Young's modulus increases 1%, to 249.3 N/m. The Poisson ratio decreases 2.6%, to 0.076. For the second-order elastic constants, C_{11} and C_{12}, the vdW effect is 1 and -1.5%, respectively. For the third-order elastic constants C_{111}, C_{112}, and C_{222}, the vdW effect is 2.5, -0.7, and 2.2%, respectively.

The in-plane stiffness of graphane is quite small compared to graphene, which indicates that the graphane is softened by the introduction of the hydrogen. This could be understood as follows. The C–C bond length in graphane is 1.54 Å, about 8.5% larger than that of graphene (1.42 Å). The C–C bonds have been stretched in graphane by the introduction of hydrogen atoms referring to the pristine graphene. These stretched C–C bonds are weaker than those unstretched, resulting a reduction of the mechanical strength.

Higher-order (>2) elastic constants are important quantities [50] and can be determined by measuring the changes of sound velocities under the application of hydrostatic and uniaxial stresses [51]. The higher-order elastic constants can be utilized to study the nonlinear elasticity, thermal expansion (through Gruneisen parameter), temperature dependence of elastic constants, harmonic generation, phonon-phonon interactions, lattice defects, phase transitions, echo phenomena, strain softening, and so on [27]. Using the higher-order elastic continuum description, one can calculate the stress and deformation state under uniaxial stress, rather than uniaxial strain. Explicitly, when pressure is applied, the pressure dependent second-order elastic moduli can be obtained from the higher-order elastic continuum description [33]. The third-order elastic constants are important in understanding the nonlinear elasticity of materials, such as changes in acoustic velocities due to finite strain. As a consequence, nano devices, such as nano surface acoustic wave sensors and nano waveguides, could be synthesized by introducing local strain [52].

Graphane monolayers exhibit instability under large tension. Stress-strain curves in the previous section show that they will soften when the strain is larger than the ultimate strain. From the view of electron bonding, this is due to the bond weakening and breaking. This softening behavior is determined by the TOECs and FFOECs from the continuum aspect. The negative values of TOECs and FFOECs ensure the softening of the graphane monolayers under large strain. The van der Waals interactions have little effect on the softening of graphane under large strains.

4. Conclusions

In summary, we studied the mechanical response of graphane under various strains using first-principles calculations based on density functional theory, with van der Waals interactions. We found that the van der Waals interactions have little effect on the geometry, ultimate strengths, ultimate strains, in-plane stiffness, and Poisson ratio. Thus, one could safely neglect the van der Waals interactions in predicting the mechanical behaviors of the graphane from the first-principles calculations. Our results might also be helpful to estimate the effect of van der Waals interactions on the mechanical properties of a large class of chemically functionalized graphene systems, including those with *s*-type, *p*-type, and *d*-type functionalization chemicals predicted from van der Waals density functional calculations.

Funding

Q.P. and S.D. would like to acknowledge the generous financial support from the Defense Threat Reduction Agency (DTRA) grant #BRBAA08-C-2-0130 and #HDTRA1-13-1-0025. Z.C. acknowledges the support by DoD grant #W911NF-12-1-0083.

References

[1] S. Grimme, Accurate description of van der Waals complexes by density functional theory including empirical corrections, J. Comput. Chem., vol. 25, no. 12, pp. 1463–1473, 2004.
[2] S. Grimme, Semiempirical GGA-type density functional constructed with a long-range dispersion correction, J. Comput. Chem., vol. 27, no. 15, pp. 1787–1799, 2006.
[3] M. Vanin, J.J. Mortensen, A.K. Kelkkanen, J.M. Garcia-Lastra, K.S. Thygesen, and K.W. Jacobsen, Graphene on metals: A van der Waals density functional study, Phys. Rev. B, vol. 81, no. 8, p. 081408, 2010.
[4] S.P. Chan, M. Ji, X.G. Gong, and Z.F. Liu, Pressure-driven confinement of hydrogen molecules between graphene sheets in the regime of van der Waals repulsion, Phys. Rev. B, vol. 69, no. 9, p. 092101, 2004.
[5] M. Bostrom and B.E. Sernelius, Repulsive van derWaals forces due to hydrogen exposure on bilayer grapheme, Phys. Rev. A, vol. 85, no. 1, p. 012508, 2012.
[6] M. Andersen, L. Hornekaer, and B. Hammer, Graphene on metal surfaces and its hydrogen adsorption: A meta-GGA functional study, Phys. Rev. B, vol. 86, no. 8, p. 085405, 2012.
[7] R. Rahman and D. Mazumdar, Ab-initio adsorption study of chitosan on functionalized graphene: Critical role of Van Der Waals interactions, J. Nanosci. Nanotech., vol. 12, no. 3, pp. 2360–2366, 2012.
[8] D.C. Elias, R.R. Nair, T.M.G. Mohiuddin, S.V. Morozov, P. Blake, M.P. Halsall, A.C. Ferrari, D.W. Boukhvalov, M.I. Katsnelson, A.K. Geim, and K.S. Novoselov, Control of graphene's properties by reversible hydrogenation: Evidence for graphane, Science, vol. 323, no. 5914, pp. 610–613, 2009.
[9] M.Z.S. Flores, P.A.S. Autreto, S.B. Legoas, and D.S. Galvao, Graphene to graphane: A theoretical study, Nanotech., vol. 20, no. 46, p. 465704, 2009.
[10] R. Balog, B. Jorgensen, L. Nilsson, M. Andersen, E. Rienks, M. Bianchi, M. Fanetti, E. Laegsgaard, A. Baraldi,

S. Lizzit, Z. Sljivancanin, F. Besenbacher, B. Hammer, T.G. Pedersen, P. Hofmann, and L. Hornekaer, Bandgap opening in graphene induced by patterned hydrogen adsorption, Nat. Mater., vol. 9, no. 4, pp. 315–319, 2010.

[11] F. Guinea, M.I. Katsnelson, and A.K. Geim, Energy gaps and a zero-field quantum Hall effect in graphene by strain engineering, Nat. Phys., vol. 6, no. 1, pp. 30–33, 2010.

[12] W. Bao, F. Miao, Z. Chen, H. Zhang, W. Jang, C. Dames, and C.N. Lau, Controlled ripple texturing of suspended graphene and ultrathin graphite membranes, Nat. Nanotech., vol. 4, no. 9, pp. 562–566, 2009.

[13] N. Gorjizadeh, A.A. Farajian, K. Esfarjani, and Y. Kawazoe, Spin and band-gap engineering in doped graphene nanoribbons, Phys. Rev. B, vol. 78, p. 155427, 2008.

[14] M. Wu, X. Wu, and X.C. Zeng, Exploration of half metallicity in edge-modified grapheme nanoribbons, J. Phys. Chem. C, vol. 114, no. 9, pp. 3937–3944, 2010.

[15] E. Kan, Z. Li, J. Yang, and J.G. Hou, Half-metallicity in edge-modified zigzag graphene nanoribbons, J. Amer. Chem. Soc., vol. 130, no. 13, pp. 4224–4225, 2008.

[16] T. Kuila, S. Bose, A.K. Mishra, P. Khanra, N.H. Kim, and J.H. Lee, Chemical functionalization of graphene and its applications, Prog. Mater. Sci., vol. 57, no. 7, pp. 1061–1105, 2012.

[17] M.H.F Sluiter and Y. Kawazoe, Cluster expansion method for adsorption: Application to hydrogen chemisorption on grapheme, Phys. Rev. B, vol. 68, no. 8, p. 085410, 2003.

[18] Q. Peng, A.K. Dearden, J. Crean, L. Han, S. Liu, X. Wen, and S. De, New materials graphyne, graphdiyne, graphone, and graphane: Review of properties, synthesis, and application in nanotechnology, Nanotechn. Sci. Appl., vol. 7, pp. 1–29, 2014.

[19] Q. Peng, J. Crean, A.K. Dearden, X. Wen, C. Huang, S.P.A. Bordas, and S. De, Defect engineering of 2D monatomic-layer materials, Mod. Phys. Lett. B, vol. 27, no. 23, p. 1330017, 2013.

[20] Y.H. Lu and Y.P. Feng, Band-gap engineering with hybrid graphane-graphene nanoribbons, J. Phys. Chem. C, vol. 113, no. 49, pp. 20841–20844, 2009.

[21] B.S. Pujari and D.G. Kanhere, Density functional investigations of defect-induced mid-gap states in graphane, J. Phys. Chem. C, vol. 113, no. 50, pp. 21063–21067, 2009.

[22] M. Topsakal, S. Cahangirov, and S. Ciraci, The response of mechanical and electronic properties of graphane to the elastic strain, Appl. Phys. Lett., vol. 96, no. 9, p. 091912, 2010.

[23] C. Lee, X. Wei, J.W. Kysar, and J. Hone, Measurement of the elastic properties and intrinsic strength of monolayer grapheme, Science, vol. 321, no. 5887, pp. 385–388, 2008.

[24] E. Cadelano, P.L. Palla, S. Giordano, and L. Colombo, Elastic properties of hydrogenated grapheme, Phys. Rev. B, vol. 82, p. 235414, 2010.

[25] E. Cadelano and L. Colombo, Effect of hydrogen coverage on the Young's modulus of grapheme, Phys. Rev. B, vol. 85, p. 245434, 2012.

[26] O. Leenaerts, H. Peelaers, A.D. Hernández-Nieves, B. Partoens, and F.M. Peeters, First-principles investigation of graphene fluoride and graphane, Phys. Rev. B, vol. 82, p. 195436, 2010.

[27] Q. Peng, C. Liang, W. Ji, and S. De, A theoretical analysis of the effect of the hydrogenation of grapheme to graphane on its mechanical properties, Phys. Chem. Chem. Phys., vol. 15, pp. 2003–2011, 2013.

[28] G. Leibfried and W. Ludwig, Theory of anharmonic effects in crystals, Solid State Physics, vol. 12, pp. 275–444, 1961.

[29] G. Kresse and J. Hafner, Ab initio molecular dynamics for liquid metals, Phys. Rev. B, vol. 47, p. 558, 1993.

[30] W. Kohn and L. J. Sham, Self-consistent equations including exchange and correlation effects, Phys. Rev., vol. 140, p. A1133, 1965.

[31] J. Perdew, K. Burke, and M. Ernzerhof, Generalized gradient approximation made simple, Phys. Rev. Lett., vol. 77, pp. 3865, 1996.

[32] R. O. Jones and O. Gunnarsson, The density functional formalism, its applications and prospects, Rev. Mod. Phys., vol. 61, p. 689–746, 1989.

[33] Q. Peng, W. Ji, and S. De, Mechanical properties of the hexagonal boron nitride monolayer: Ab initio study, Comput. Mater. Sci., vol. 56, pp. 11–17, 2012.

[34] Q. Peng, W. Ji, and S. De, Mechanical properties of graphyne monolayer: A first-principles study, Phys. Chem. Chem. Phys., vol. 14, pp. 13385–13391, 2012.

[35] Q. Peng, C. Liang, W. Ji, and S. De, A first principles investigation of the mechanical properties of g-TlN, Model. Numer. Simul. Mater. Sci., vol. 2, pp. 76–84, 2012.

[36] Q. Peng, C. Liang, W. Ji, and S. De, A first principles investigation of the mechanical properties of g-ZnO: The graphene-like hexagonal zinc oxide monolayer, Comput. Mater. Sci., vol. 68, pp. 320–324, 2013.

[37] Q. Peng, W. Ji, and S. De, First-principles study of the effects of mechanical strains on the radiation hardness of hexagonal boron nitride monolayers, Nanoscale, vol. 5, pp. 695–703, 2013.

[38] Q. Peng, X.-J. Chen, S. Liu, and S. De, Mechanical stabilities and properties of graphene-like aluminum nitride predicted from first-principles calculations, RSC Adv., vol. 3, pp. 7083–7092, 2013.

[39] Q. Peng, C. Liang, W. Ji, and S. De, A first-principles study of the mechanical properties of g-GeC, Mech. Mater., vol. 64, pp. 135–141, 2013.

[40] Q. Peng, X.-J. Chen, W. Ji, and S. De, Chemically tuning mechanics of graphene by BN, Adv. Eng. Mater., vol. 15, pp. 718–727, 2013.

[41] Q. Peng, C. Liang, W. Ji, and S. De, Mechanical properties of g-GaN: A first principles study, Appl. Phys. A, vol. 13, pp. 483–490, 2013.

[42] Q. Peng, X. Wen, and S. De, Mechanical stabilities of silicene, RSC Adv., vol. 3, pp. 13772–13781, 2013.

[43] Q. Peng and S. De, Outstanding mechanical properties of monolayer MoS_2 and its application in elastic energy storage, Phys. Chem. Chem. Phys., vol. 15, no. 44, pp. 19427–19437, 2013.

[44] Q. Peng and S. De, Mechanical properties and instabilities of ordered graphene oxide C_6O monolayer, RSC Adv., vol. 3, no. 46, pp. 24337–24344, 2013.

[45] Q. Peng and S. De, Elastic limit of silicone, Nanoscale, vol. 6, pp. 12071–12079, 2014.

[46] Q. Peng, L. Han, X. Wen, S. Liu, Z. Chen, J. Lian and S. De, Mechanical properties and stabilities of α-Boron monolayers, Phys. Chem. Chem. Phys., vol. 17, pp. 2160–2168, 2015.

[47] Q. Peng, L. Han, X. Wen, S. Liu, Z. Chen, J. Lian and S. De, Mechanical properties and stabilities of g-ZnS monolayers, RSC Adv., vol. 5, pp. 11240–11247, 2015.

[48] H. Sahin, C. Ataca, and S. Ciraci, Electronic and magnetic properties of graphane nanoribbons, Phys. Rev. B, vol. 81, no. 20, p. 205417, 2010.

[49] X.-D. Wen, T. Yang, R. Hoffmann, N.W. Ashcroft, R.L. Martin, S.P. Rudin, and J.-X. Zhu, Graphane nanotubes, ACS Nano, vol. 6, no. 8, pp. 7142–7150, 2012.

[50] Y. Hiki, Higher-order elastic-constants of solids, Ann. Rev. Mater. Sci., vol. 11, p. 51, 1981.

[51] K. Brugger, Determination of 3rd-order elastic coefficients in crystals, J. Appl. Phys., vol. 36, no. 3P1, p. 768, 1965.

[52] Q. Peng, A.R. Zamiri, W. Ji, and S. De, Elastic properties of hybrid graphene/boron nitride monolayer, Acta Mechanica, vol. 223, pp. 2591–2596, 2012.